Kernel-based parametric analytical model of source intensity distributions in lithographic tools

Shiyuan Liu,[1,2,*] Wei Liu,[1] Xinjiang Zhou,[1] and Peng Gong[1]

[1]Wuhan National Laboratory for Optoelectronics, Huazhong University of Science and Technology, Wuhan 430074, China

[2]State Key Laboratory of Digital Manufacturing Equipment and Technology, Huazhong University of Science and Technology, Wuhan 430074, China

*Corresponding author: shyliu@mail.hust.edu.cn

Received 24 October 2011; revised 10 December 2011; accepted 11 December 2011; posted 13 December 2011 (Doc. ID 157022); published 23 March 2012

This paper proposes a parametric analytical source model for overall representation of the physical distribution property of partially coherent illumination sources in lithographic tools. A set of smooth kernels is adopted to construct the analytical model for the multiple mainstream illumination sources. Corrected parametrical terms are subsequently presented for characterization of different physical distortions of and deviations from actual illumination sources. The corrected parametrical terms can be decomposed into Fourier series, which have special physical meanings of respectively indicating different distortion types, including shift of the center, tilt, and ellipticity, etc. We fully expected that the proposed analytical model will provide both simulation conditions and a theoretical basis for the resolution enhancement technique and related research fields. © 2012 Optical Society of America

OCIS codes: 110.5220, 110.4980, 110.2990, 230.6080.

1. Introduction

The illumination source is one of the critical components in optical lithography tools [1]. As the limit of optical lithography is pushed and feature densities continue to increase, partially coherent illumination has been widely used for improving the yield of manufacturing products [2,3]. In general, the coherence of a system is defined as the virtual image of the light source in the pupil plane of the projection optics [4]. It is also referred to as the pupil illumination function [5]. Partially coherent illumination sources are integrated into lithography as various types, including the most commonly used circular, annular, dipole, and quadrupole sources [5]. Nowadays, the traditional top-hat approximation for the pupil illumination function is used as the most convenient simulation input in resolution enhancement techniques as well as in other related research fields, such as optical proximity correction [6], fast aerial image calculation [7], and lens aberration measurement [8]. By using this kind of approximation, the pupil illumination function becomes a binary intensity distribution, which is a constant and uniform normalized intensity of one for all bright areas, and zero intensity for the remainder [9]. However, the actual illumination sources used in real-world lithographic tools always deviate significantly from a simple top-hat distribution characterized only by the partial coherence factor [10,11]; instead, they are smooth distributions with different kinds of distortions. The unrealistic assumption of a top-hat instead of the actual illumination pupil fill will lead to a loss in accuracy of the optical component during the process simulation. This impact becomes even more important with increasingly sophisticated layout-specific illuminations for low k1 lithography. Therefore, manufacturers of lithographic tools need to develop a more accurate model to approximate

1559-128X/12/101479-08$15.00/0

and characterize the actual source intensity distributions.

Various methods for characterization of source distributions have been investigated. Barouch *et al.* proposed a contour-based representation method [12] in which every point inside the contour is assumed to have a brightness of one, and a brightness of zero outside the contour. Barrett reported a method to represent the source intensity distributions by multiple parameters [13], including the base sigma, side angle, center drop, and imbalance parameters, so that the illumination sources could be constructed as a combination of primary shapes such as circles and rectangles. Although these methods have a more flexible form than the traditional top-hat approximation approach characterized only by the partial coherence factor, the more important limitation still remains, as the resulting source intensity distributions are not smooth. To overcome this drawback, the pixel-based representation seems to provide another good choice, as it is a straightforward method with the most flexible representational ability [14]. However, this representation lacks any physical meaning in interpreting the source intensity distributions, and a large number of pixels have to be used to accurately model an actual illumination source, which in turn leads to a very large dimensionality in the actual source optimization. Recently, Granik and Adam proposed an analytical approximation model to characterize the standard, annular, dipole, and quadrupole sources with smooth distributions [15]. This model is based on a smooth kernel and can be considered as an efficient compression of the source intensity information; thus, it does not need to handle the large amount of data encountered in the pixel-based representation. As the analytical model is simply constructed using radially symmetric functions, this method is limited to approximating and characterizing radially symmetric intensity distributions, and it is not suitable for spatially variable intensity distributions with asymmetric distortions. Flagello *et al.* also reported an analytical smooth source model with nearly 20 parameters to describe different kinds of intensity distortions [16]. Matsuyama *et al.* proposed a pupilgram modulation model expressed by linear combinations of Zernike intensity modulation functions and Zernike distortion modulation functions [17]. Although these two different models have the same advantage of separating the geometric shape from the power distributions, they are somewhat inconvenient when used in rapidly setting up and fitting actual intensity distributions, as both of the models have a complicated analytical expression with several cumbersome numerical integrations or with summations of multiple Zernike polynomials.

In this paper, we attempt to make improvements on both Granik and Adam's method and Flagello *et al.*'s approach, and we propose a parametric analytical model in a compact form with a simplest expression for overall representation of the physical distribution property of partially coherent illumination sources in lithographic tools. We adopt a set of smooth kernels to construct the analytical model for the multiple mainstream illumination sources, and then we present several corrected parametric terms to characterize different physical distortions of and deviations from source intensity distributions. The corrected parametric terms can be decomposed into Fourier series, which have special physical meanings that indicate different distortion types, including shift of the center, tilt, and ellipticity.

2. Theory

Because the light power generated by the laser beam from the illumination source tends to continuously decay in its propagation, the actual illumination intensity used in real-world lithographic tools always deviates significantly from a simple top-hat distribution. In this paper, we introduce a set of one-dimensional kernel functions for modeling analytical continuous intensity distributions. It is convenient to streamline the ingredient step functions by convoluting the Heaviside step function with the Gaussian kernel of diffusion length g:

$$K_g(x) = \frac{1}{\sqrt{\pi}g}\mathrm{Step}(x) \otimes \exp\left(\frac{x^2}{g^2}\right). \tag{1}$$

Here, the step function is expressed as

$$\mathrm{Step}(x) = \begin{cases} 1, & x \geq 0 \\ 0, & x < 0 \end{cases}, \tag{2}$$

which results in the following expression with the *erf* function:

$$K_g(x) = \frac{1}{2} + \frac{1}{2}erf\left(\frac{x}{g}\right). \tag{3}$$

The *erf* function is defined as

$$erf(x) = \frac{2}{\sqrt{\pi}}\int_0^x e^{-t^2}\mathrm{d}t. \tag{4}$$

Similarly, we can also construct smooth kernels by using the following analytical functions:

$$K_P(x) = \frac{1}{2} + \frac{1}{2}\frac{x}{\sqrt{P^2 + x^2}}, \tag{5}$$

$$K_t(x) = \frac{1}{2} + \frac{1}{\pi}\arctan\left(\frac{\pi}{2t}x\right), \tag{6}$$

$$K_h(x) = \frac{1}{2} + \frac{1}{2}\tanh\left(\frac{x}{h}\right). \tag{7}$$

Here, $\tanh(x)$ is known as the hyperbolic function. To conclude, $K_g(x)$, $K_p(x)$, $K_t(x)$, and $K_h(x)$ are different smooth kernels that are proposed for

approximating continuous intensity distributions. g, p, t, and h are selected as smooth parameters of the corresponding kernels. Figure 1 compares these proposed kernels when $g = 0.3$, $p = 0.5$, $t = 1$, and $h = 3$. It also shows that $K_g(x)$, $K_p(x)$, $K_t(x)$, and $K_h(x)$ can be considered a set of kernels having the same property of a continuous S-shape distribution. This set of kernels can therefore be used instead of the traditional step function for modeling the analytical intensity distribution. To make notation more compact, in this paper we use one kernel, the $K_p(x)$ function, as an example for further proposing the parametric analytical source model.

For circular or annular sources with radially symmetric intensity distributions, the continuous intensity distributions can be modeled by the proposed smooth kernel with the expressions of

$$I_C(r) = K_P(\sigma - r), \tag{8}$$

$$I_A(r) = K_{P_o}(\sigma_o - r) \cdot K_{P_i}(r - \sigma_i), \tag{9}$$

where $I_C(r)$ and $I_A(r)$ indicate the circular source and annular source, respectively. σ is the partial coherence factor for circular source. σ_i and σ_o represent partial coherence factors for the outer and inner circles of an annular source. From Eqs. (8) and (9), the circular and annular sources are treated as a combination of light regions that are only defined by radius r in polar coordinates (r, θ). Moreover, the dipole or quadrupole sources can be considered as two or four sections of the corresponding annular source that are limited in the azimuthal direction. Therefore, dipole and quadrupole sources with radially symmetric intensity distributions are expressed as

$$I_D(r,\theta) = I_A(r)T_D(\theta), \tag{10}$$

$$I_Q(r,\theta) = I_A(r)T_Q(\theta). \tag{11}$$

Here, $I_D(r)$ and $I_Q(r)$ indicate the dipole source and quadrupole source, respectively. $T_D(\theta)$ and $T_Q(\theta)$ indicate the limited sections for dipole and quadrupole sources in the azimuthal direction by angle θ_0, and can be therefore written as the following kernel-based expressions:

$$T_D(\theta) = K_{P_\theta}(\theta_0 - |\theta|) + K_{P_\theta}(\theta_0 - |\pi - \theta|), \tag{12}$$

$$\begin{aligned} T_Q(\theta) = {} & K_{P_\theta}\left(\theta_0 - \left|\frac{\pi}{4} - \theta\right|\right) + K_{P_\theta}\left(\theta_0 - \left|\frac{3\pi}{4} - \theta\right|\right) \\ & + K_{P_\theta}\left(\theta_0 - \left|\frac{5\pi}{4} - \theta\right|\right) + K_{P_\theta}\left(\theta_0 - \left|\frac{7\pi}{4} - \theta\right|\right). \end{aligned} \tag{13}$$

From Eqs. (8)–(13), the source models with continuous intensity distributions are straightforward improvements of traditional top-hat sources. It is also beneficial to extend the analytical source models with radially symmetric intensity distributions to a more general case of spatially variable intensity distributions of different distortions. The corrected parametric terms are thus proposed to accomplish this based on Eqs. (8) and (9):

$$I_C^*(x,y) = [1 + \alpha(\theta^*)]K_P[\sigma - r^* + \gamma(\theta^*)], \tag{14}$$

$$\begin{aligned} I_A^*(x,y) = {} & [1 + \alpha(\theta^*)] \cdot K_{P_o}[\sigma_o - r^* + \gamma(\theta^*)] \\ & \cdot K_{P_i}[r^* - \sigma_i + \beta(\theta^*)], \end{aligned} \tag{15}$$

where (x, y) are Cartesian coordinates corresponding to polar ones (r, θ). $I_C^*(x,y)$ and $I_A^*(x,y)$ are corrected source intensities for circular and annular sources. (r^*, θ^*) are corrected polar coordinates expressed by

$$r^* \cos(\theta^*) = x - x_0, r^* \sin(\theta^*) = y - y_0. \tag{16}$$

Here, (x_0, y_0) represents the pupil shifts (center shift of the source intensities related to the pupil) in x/y directions. $\alpha(\theta^*)$, $\beta(\theta^*)$ and $\gamma(\theta^*)$ are corrected parametric terms which can be decomposed by Fourier series up to the second order. $\alpha(\theta^*)$ is the corrected term for power shifts. $\beta(\theta^*)$ and $\gamma(\theta^*)$ are corrected terms for geometric shifts:

$$\begin{aligned} \alpha(\theta^*) = {} & [a_{\alpha 1} \cos(\theta^*) + b_{\alpha 1} \sin(\theta^*)] \\ & + [a_{\alpha 2} \cos(2\theta^*) + b_{\alpha 2} \sin(2\theta^*)], \end{aligned} \tag{17}$$

$$\begin{aligned} \beta(\theta^*) = {} & [a_{\beta 1} \cos(\theta^*) + b_{\beta 1} \sin(\theta^*)] \\ & + [a_{\beta 2} \cos(2\theta^*) + b_{\beta 2} \sin(2\theta^*)], \end{aligned} \tag{18}$$

$$\begin{aligned} \gamma(\theta^*) = {} & [a_{\gamma 1} \cos(\theta^*) + b_{\gamma 1} \sin(\theta^*)] \\ & + [a_{\gamma 2} \cos(2\theta^*) + b_{\gamma 2} \sin(2\theta^*)]. \end{aligned} \tag{19}$$

From Eq. (15), the corrected intensities for dipole and quadrupole sources can be expressed as follows:

$$I_D^*(r,\theta) = I_A^*(r,\theta)T_D(\theta), \tag{20}$$

$$I_Q^*(r,\theta) = I_A^*(r,\theta)T_Q(\theta), \tag{21}$$

where $I_D^*(x,y)$ and $I_Q^*(x,y)$ are corrected intensities for dipole and quadrupole sources. Normalize $I_C^*(x,y)$, $I_A^*(x,y)$, $I_D^*(x,y)$, and $I_Q^*(x,y)$ to $J_C(x,y)$, $J_A(x,y)$, $J_D(x,y)$, and $J_Q(x,y)$ by

$$J_C(x,y) = I_C^*(x,y)/\max[I_C^*(x,y)], \tag{22}$$

$$J_A(x,y) = I_A^*(x,y)/\max[I_A^*(x,y)], \tag{23}$$

$$J_D(x,y) = I_D^*(x,y)/\max[I_D^*(x,y)], \quad (24)$$

$$J_Q(x,y) = I_Q^*(x,y)/\max[I_Q^*(x,y)]. \quad (25)$$

From Eqs. (22)–(25), the maximum intensities of $J_C(x,y), J_A(x,y), J_D(x,y)$, and $J_Q(x,y)$ are all normalized to unit one. $J_C(x,y), J_A(x,y), J_D(x,y)$, and $J_Q(x,y)$ can thus be proposed as a kernel-based parametric analytical model for spatially variable intensity distributions.

According to Eqs. (1)–(13), the smooth analytical source functions are preconditions of obtaining the parametric source model. We note that this set of kernels is different from that proposed in [15]. Based on the expressions of the traditional top-hat source model, this smooth source model is similar to the model in [15], but not exactly the same. The proposed parametric source model can be considered an improvement of the method in [15]. Moreover, like the method reported in [16], the proposed parametric source model also uses Fourier series expansion to indicate intensity distortions, but has a compact form with a simplest expression and no cumbersome numerical integration. Therefore, the proposed parametric source model is a direct improvement of the method in [16], and the orthogonality of the proposed corrected parametric terms will lead to a high accuracy when actual source intensities are fitted.

3. Parametric Source Simulation

To simulate the parametric source model, we compared of mainstream sources radially symmetric intensity distributions and top-hat distributions of mainstream source. From Eqs. (8)–(11), Fig. 2 shows the simulation result with the setting conditions of circular source ($\sigma = 0.31$), annular source ($\sigma_o/\sigma_i = 0.7/0.4$), dipole source ($\sigma_o/\sigma_i/\theta_0 = 0.7/0.4/22.5°$), and quadrupole source ($\sigma_o/\sigma_i/\theta_0 = 0.7/0.4/22.5°$) using the smooth parameters $P_o = P_i = P_\theta = 0.07$. We show that the kernel-based smooth presentation successfully provides the mainstream sources with continuous intensity distributions and becomes more flexible than the traditional top-hat representation.

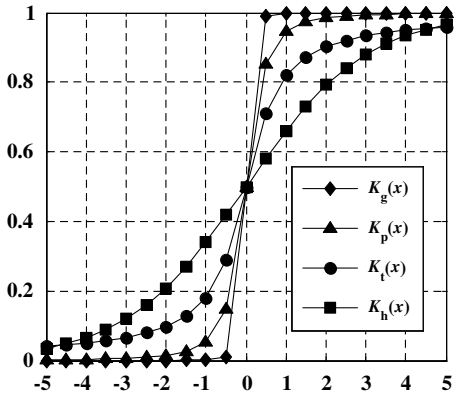

Fig. 1. Set of smooth kernels with $g = 0.3$, $p = 0.5$, $t = 1$, and $h = 3$.

For simplicity's sake, the simulation of the parametric model is concentrated on an annular source, but the concepts and models have been developed for multiple illumination shapes including circular, dipole, and quadrupole sources. From Eqs. (15)–(19), the parametric model for the annular source has, overall, 18 parameters to represent the spatially variable intensity distributions. The advantage of this model is that it separates effects on the geometric shift in the source shape from the power distributions. It includes four primary parameters: σ_i (inner radius), σ_o (outer radius), P_i (inner slope of the annulus), and P_o (outer slope of the annulus). Figure 3 shows the effects of corrected parameters on power shifts (or intensity shifts). Figure 4 shows the effects of corrected parameters on the geometric shifts. As illustrated in Figs. 3 and 4, the physical meanings of corrected parameters for geometric shifts and power shifts can be summarized as follows: parameters $a_{\alpha 1}$ and $b_{\alpha 1}$ indicate a power tilt in x direction and y direction; parameters $a_{\alpha 2}$ and $b_{\alpha 2}$ indicate power horizontal and vertical (HV) ellipticity and slanting and tilting (ST) ellipticity; parameters $a_{\beta 1}$ and $a_{\gamma 1}$ indicate an x shift of the center for the inner ring and the outer ring; parameters $b_{\beta 1}$ and $b_{\gamma 1}$ indicate a y shift of the center for the inner circle and outer circle; parameters $a_{\beta 2}$ and $a_{\gamma 2}$ indicate geometric HV ellipticity of the inner ring and the outer ring; parameters $b_{\beta 2}$ and $b_{\gamma 2}$ indicate geometric ST ellipticity of the inner ring and the outer ring.

4. Experimental Source Fitting

We used the annular parametric model to fit the measured reference sources under different illumination settings in an experimental lithographic tool provided by Shanghai Micro Electronics Equipment (SMEE) Corporation, with NA = 0.75 and wavelength = 193 nm. The measured reference sources shown in Fig. 5 can be obtained by a transmission image sensor (TIS) scanning in a lateral plane at a certain defocus [18]. The best fit was achieved by operating on a 2.53 GHz Opteron workstation with MATLAB in Windows 7 (64-bit), using the least-squares minimization algorithm. A one-time experimental source fitting took only 0.076 s (the pixel number of the fitted sources is 1521).

Figure 6 shows the fitted result under the measured source 1, which has a complete intensity distribution in the pupil plane. From Fig. 6, all the fitted errors around the pupil plane tend to be in a random distribution and to converge within ±0.1 (the maximum intensity value is normalized). Figure 7 shows the fitted result under the measured source 2, which has a very large center shift on the pupil plane. Although the reference-measured source 2 is not a whole annular shape, but is an incomplete distribution in the pupil plane, Fig. 7 shows that the

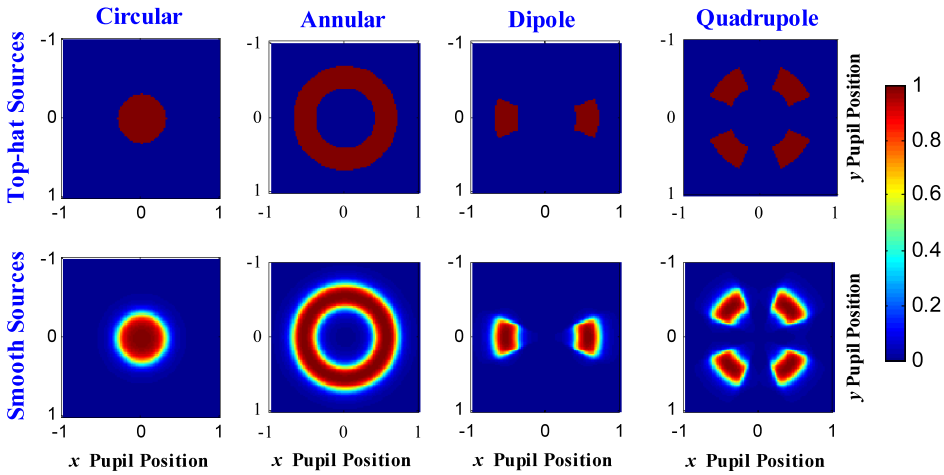

Fig. 2. (Color online) Comparison of mainstream sources between radially symmetric intensity distributions and top-hat distributions, under the simulation conditions of circular source ($\sigma = 0.31$), annular source ($\sigma_o/\sigma_i = 0.7/0.4$), dipole source ($\sigma_o/\sigma_i/\theta_0 = 0.7/0.4/22.5°$), and quadrupole source ($\sigma_o/\sigma_i/\theta_0 = 0.7/0.4/22.5°$) using smooth parameters $P_o = P_i = P_\theta = 0.07$.

maximum error of the fitted source is also less than 0.1. This demonstrates, therefore, that the proposed parametric source model is not only accurate and efficient for fitting sources with complete distributions, it is also well-correlated with the measured sources of seriously incomplete shapes.

Figure 8 shows the comparison of fitted results using the proposed parametric source model and the traditional top-hat model under the measured source 3. It shows that the fitted accuracy is greatly improved by using the proposed parametric source model when considering influences of different distortions on actual intensity distributions. Note in Figs. 6–8 that the absolute fitted errors of source intensities are on the order of 0.01 (the maximum intensity is normalized to 1). Given the inevitable errors induced by the performance of actual source metrology, the fitted results demonstrate that the proposed parametric source model yields superior characterizations of the intensity distributions of actual illuminations.

To show the benefit of the proposed parametric source model, we can also introduce the metric of source map similarity, for evaluating the difference between the measured source and fitted source [15]. The similarity, M, of two source maps, S_1 and S_2, is defined as 1 minus the ratio of their difference to norm −1 of their sum:

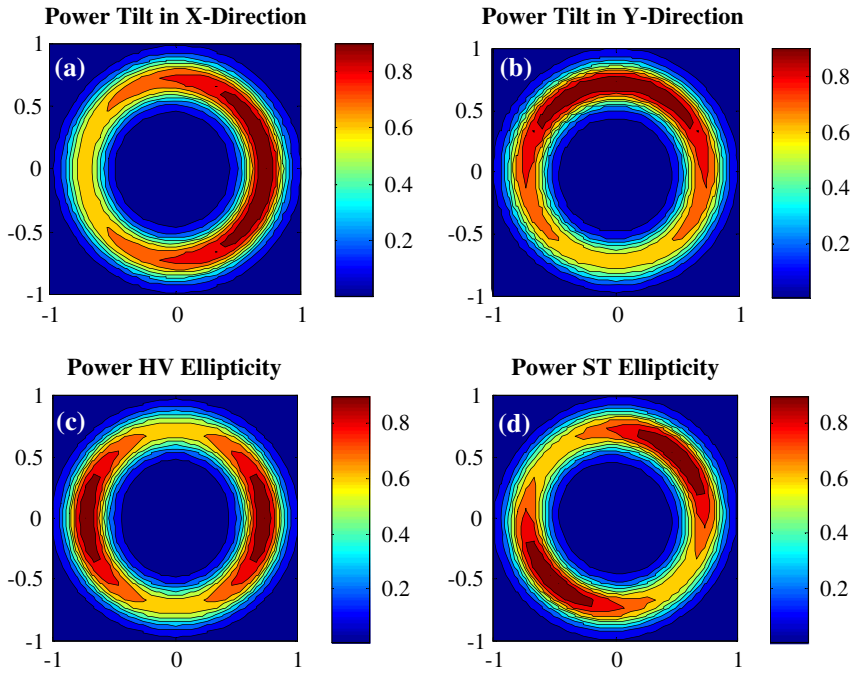

Fig. 3. (Color online) Examples of the kernel-based parametric analytical model in characterizing the effects on different kind of power shifts of an annular source ($\sigma_o/\sigma_i = 0.85/0.6$) under the smooth parameters $P_o = P_i = 0.1$: (a) power tilt in X-direction ($a_{a1} = 0.2$), (b) power tilt in Y-direction ($b_{a1} = 0.2$), (c) power HV ellipticity ($a_{a2} = 0.2$), and (d) power ST ellipticity ($b_{a2} = 0.2$).

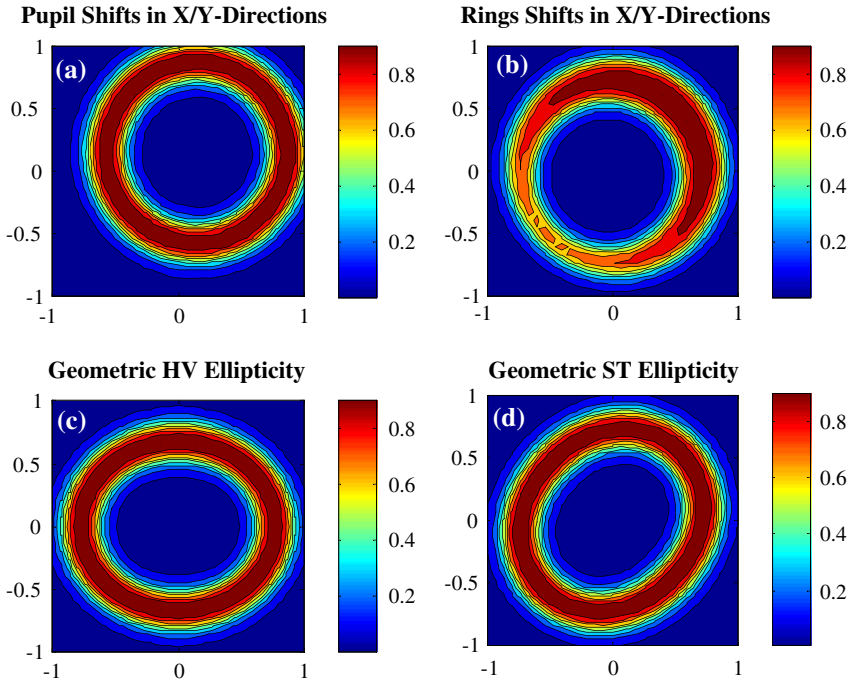

Fig. 4. (Color online) Examples of the kernel-based parametric analytical model in characterizing the effects on different kind of geometric shifts of an annular source ($\sigma_o/\sigma_i = 0.85/0.6$) under the smooth parameters $P_o = P_i = 0.1$: (a) pupil shifts in X/Y-directions ($x_0 = 0.15$, and $y_0 = 0.15$), (b) rings shifts in X/Y-directions ($a_{\beta 1} = 0.07$, $a_{\gamma 1} = 0.07$, $b_{\beta 1} = 0.07$, and $b_{\gamma 1} = 0.07$), (c) geometric HV ellipticity ($a_{\beta 2} = -0.05$, and $a_{\gamma 2} = 0.05$), and (d) geometric ST ellipticity ($b_{\beta 2} = -0.05$, and $b_{\gamma 2} = 0.05$).

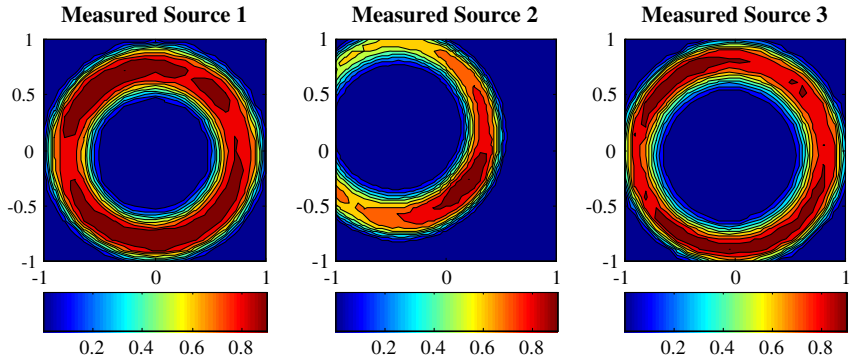

Fig. 5. (Color online) Measured reference sources under different illumination settings: Measured Source 1 ($\sigma_o/\sigma_i = 0.95/0.6$), Measured Source 2 ($\sigma_o/\sigma_i = 0.9/0.65$), and Measured Source 3 ($\sigma_o/\sigma_i = 0.97/0.7$).

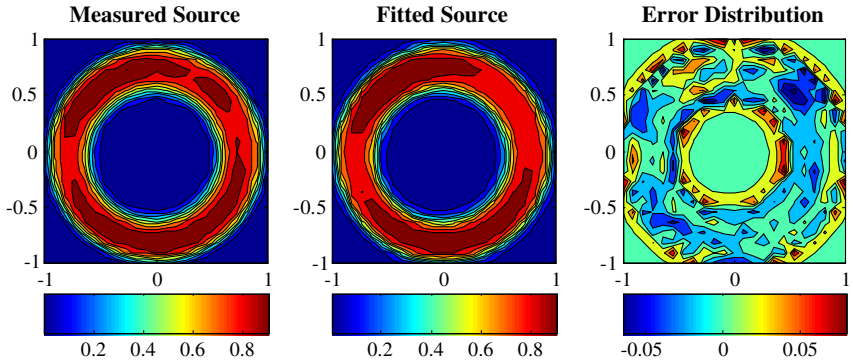

Fig. 6. (Color online) Illustration of measured and fitted annular source: source intensity distribution is complete in the pupil plane.

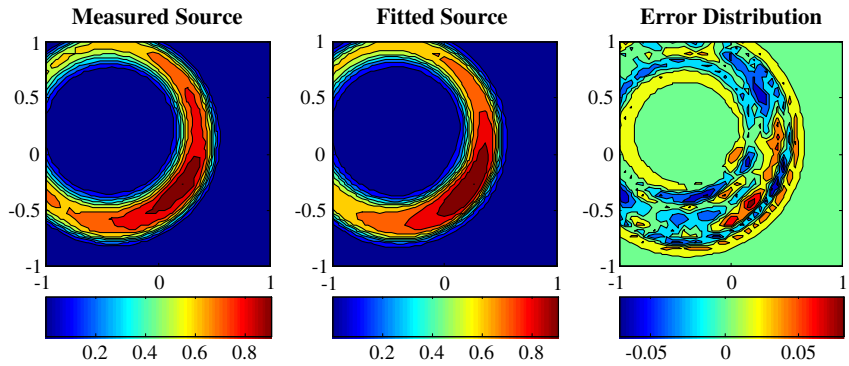

Fig. 7. (Color online) Illustration of measured and fitted annular source: source intensity distribution is incomplete in the pupil plane.

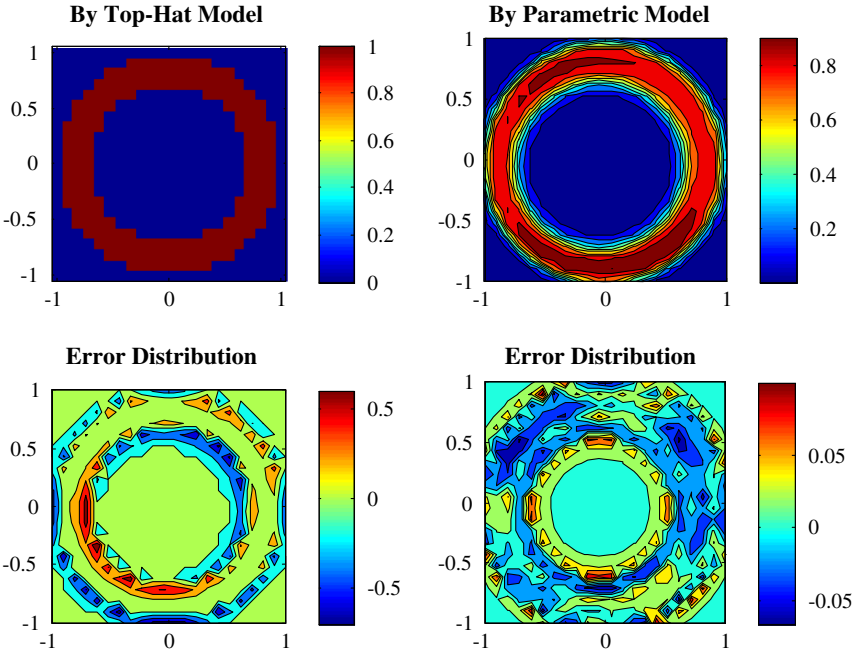

Fig. 8. (Color online) Comparison of fitted results by using the proposed parametric source model and the traditional top-hat model for the Measured Source 3.

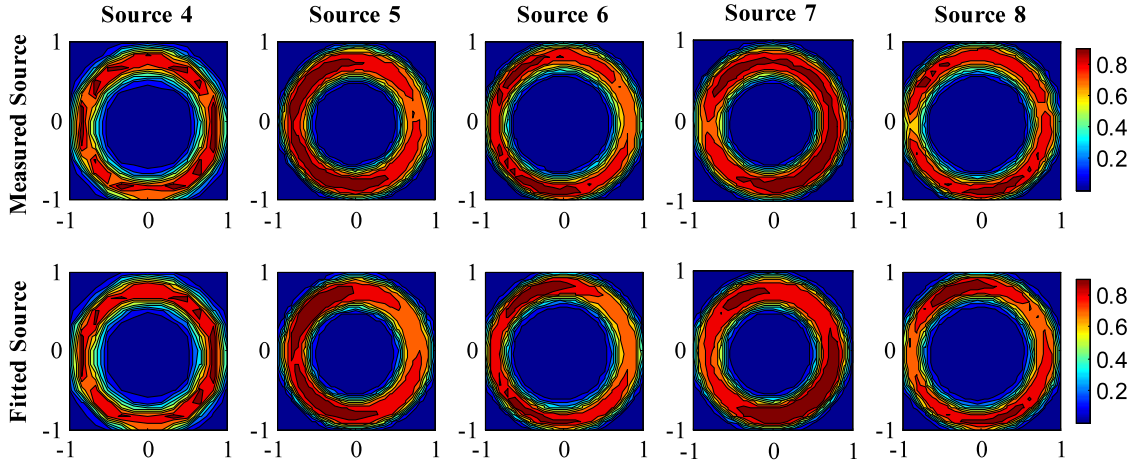

Fig. 9. (Color online) Comparison between measured and fitted annular sources under different illumination settings.

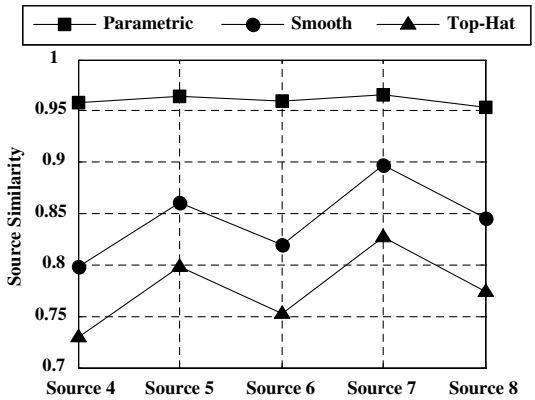

Fig. 10. Similarity values of measured and fitted sources by using different fitting models, including the parametric source model, smooth source model, and the top-hat source model.

$$M(S_1, S_2) = 1 - \frac{\|S_2 - S_1\|_1}{\|S_2 + S_1\|_1} = 1 - \frac{\iint |S_2 - S_1| \mathrm{d}x\mathrm{d}y}{\iint |S_2 + S_1| \mathrm{d}x\mathrm{d}y}. \tag{26}$$

We also fitted other measured annular sources under different pupil settings based on the proposed parametric source model. Figure 9 compares measured and fitted annular sources from Source 4 to Source 8, using the parametric source model. Nevertheless, we adopted the smooth source model using Eq. (9) and the top-hat source model to fit these sources. Figure 10 illustrates the similarity values of measured and fitted sources by using different fitting models. Figure 10 shows that the parametric source model achieves larger values of similarity compared to the smooth source model or the top-hat source model. The percentage gain in similarity when going from the smooth model to the parametric source model is more than 7%, which demonstrates that the parametric source model better matches the actual sources by utilizing the corrected parametric terms. The high similarity, greater than 95%, indicates that the CD difference through pitch when comparing to the simulation with the measured source map will be smaller [15]. The parametric model will, therefore, be more accurate in the optical simulation, which has direct benefits in model-based resolution enhancement techniques.

5. Conclusions

Actual illumination sources used in real-world lithographic tools always deviate significantly from a simple top-hat distribution characterized only by the partial coherence factor; instead, they are spatially variable intensity distributions with different kinds of distortions. This paper proposes a kernel-based parametric analytical source model for overall representation of the physical distribution property of partially coherent illumination sources in lithographic tools. Corrected parametrical terms are adopted in the kernel-based parametric analytical source model for accurately representing multiple physical distortions of and deviations from actual illumination sources. According to the simulation and experimental results, the proposed analytical model has been proved to be simple to implement and to yield a superior quality of actual source fitting. Hence, it may provide both simulation conditions and a theoretical basis for resolution enhancement techniques and related research fields.

This work was supported by National Natural Science Foundation of China (grant nos. 91023032 and 51005091). The authors thank the National Engineering Research Center for Lithographic Equipment of China for supporting this work.

Reference

1. F. M. Schellenberg, "A history of resolution enhancement technology," Opt. Rev. **12**, 83–89 (2005).
2. A. K. Wong, *Optical Imaging in Projection Microlithography* (SPIE, 2005), Chap. 4.
3. B. J. Lin, *Optical Lithography: Here is Why* (SPIE, 2010), Chap. 3.
4. E. Wolf, "New spectral representation of random sources and of the partially coherent fields that they generate," Opt. Commun. **38**, 3–6 (1981).
5. G. Perçin, A. Sezginer, and F. X. Zach, "Metrology for stepper illumination pupil profile," J. Micro/nanolithogr. MEMS MOEMS **5**, 023006 (2006).
6. X. Ma and G. R. Arce, "PSM design for inverse lithography with partially coherent illumination," Opt. Express **16**, 20126–20141 (2008).
7. K. Yamazoe, "Fast fine-pixel aerial image calculation in partially coherent imaging by matrix representation of modified Hopkins equation," Appl. Opt. **49**, 3909–3915 (2010).
8. W. Liu, S. Y. Liu, T. T. Zhou, and L. J. Wang, "Aerial image based technique for measurement of lens aberrations up to 37th Zernike coefficient in lithographic tools under partial coherent illumination," Opt. Express **17**, 19278–19291 (2009).
9. C. Bodendorf, R. E. Schlief, and R. Ziebold, "Impact of measured pupil illumination fill distribution on lithography simulation and OPC models," Proc. SPIE **5377**, 1130–1145 (2004).
10. J. Shin, C. Hwang, S. Lee, S. Woo, H. Cho, and J. Moon, "Understanding the impact of source displacement error on sub-90 nm patterns using a fresnel zone plate," J. Vac. Sci. Technol. B **23**, 2653–2656 (2005).
11. W. Liu, S. Y. Liu, T. L. Shi, and Z. R. Tang, "Generalized formulations for aerial image based lens aberration metrology in lithographic tools with arbitrarily shaped illumination sources," Opt. Express **18**, 20096–20104 (2010).
12. E. Barouch, S. L. Knodle, S. A. Orszag, and M. Yeung, "Illuminator optimization for projection printing," Proc. SPIE **3679**, 697–703 (1999).
13. T. C. Barrett, "Impact of illumination pupil-fill spatial variation on simulated imaging performance," Proc. SPIE **4000**, 804–817 (2000).
14. Y. Granik, "Source optimization for image fidelity and throughput," J. Micro/nanolithogr. MEMS MOEMS **3**, 509–522 (2004).
15. Y. Granik and K. Adam, "Analytical approximations of the source intensity distributions," Proc. SPIE **5992**, 599255 (2005).
16. D. G. Flagello, B. Geh, R. Socha, P. Liu, Y. Cao, R. Stas, O. Natt, and J. Zimmermann, "Understanding illumination effects for control of optical proximity effects (OPE)," Proc. SPIE **6924**, 69241U (2008).
17. T. Matsuyama, N. Kita, and Y. Mizuno, "Pupilgram adjusting scheme using intelligent illuminator for ArF immersion exposure tool," Proc. SPIE **7973**, 79731H (2011).
18. H. van der Laan, M. Dierichs, H. van Greevenbroek, E. McCoo, F. Stoffels, R. Pongers, and R. Willekers, "Aerial image measurement methods for fast aberration setup and illumination pupil verification," Proc. SPIE **4346**, 394–407 (2001).